Kidney International, Vol. 58 (2000), pp. 1300–1310

Magnetic resonance imaging detection of rat renal transplant rejection by monitoring macrophage infiltration

YUQING ZHANG, STEPHEN J. DODD, KRISTY S. HENDRICH, MANGAY WILLIAMS, and CHIEN HO

Pittsburgh NMR Center for Biomedical Research and Department of Biological Sciences, Carnegie Mellon University, Pittsburgh, Pennsylvania, USA

Magnetic resonance imaging detection of rat renal transplant rejection by monitoring macrophage infiltration.

Background. A rat renal transplantation model was studied by noninvasive magnetic resonance imaging (MRI) with an infusion of ultrasmall superparamagnetic iron oxide (USPIO) particles to test whether the accumulation of immune cells, such as macrophages, could be detected in vivo while the kidney transplant was being rejected.

Methods. Major histocompatibility disparate DA to BN male rat renal transplantation recipients were infused with USPIO particles, with magnetic resonance (MR) images acquired before, immediately after, and one day following infusion.

Results. When the USPIO infusion was on the fourth day post-transplantation, some rejecting allografts showed a decrease of MR signal intensity one day later. Isografts and allografts with triple immunosuppressant treatment had no MR signal reduction. Immunohistologic staining for $ED1^+$ macrophages and $CD4^+$ and $CD8^+$ T cells in allogeneic transplanted kidneys indicated the accumulation of these immune cells as acute rejection occurred. Morphological studies by electron microscopy confirmed the existence of iron inside the lysosomes of macrophages of rejecting kidneys, while Prussian blue staining detected the presence of iron plaques in macrophages. Isografts and allografts with a triple immunosuppressant treatment exhibited smaller MR signal reductions with minimal histologic changes.

Conclusions. The concurrence of MR signal reduction following USPIO infusion with pathological manifestation in a rat renal allograft model suggests the possibility that renal transplantation status may be assessed by MRI using USPIO particles as markers for the accumulation of immune cells, such as macrophages.

Renal transplantation is a commonly preferred surgical procedure for patients with end-stage nonmalignant renal disease [1, 2]. It is now recognized to be the most effective treatment because it offers the best prognosis (that is, over a 70% 5-year survival rate with kidney transplantation from living-related donors), a superior quality of life (as compared with hemodialysis or peritoneal dialysis), and improved rehabilitation. For a review of kidney transplantation, refer to Racusen, Solez, and Burdick [2]. Long-term survival is still threatened by repeated episodes of acute rejection and by chronic rejection. Through renal biopsies, it has been found that as many as 30% of all renal transplantation cases develop rejection within one year, even with the intervention of various immunosuppressive regimens. Other potential complications of renal transplants include infection caused by immunosuppression, nephrotoxicity, etc. [3]. Clinically, chronic rejection of renal transplants, like most other solid organ transplants, is the leading cause of late allograft failure. Although the pathophysiological mechanism of chronic rejection remains poorly understood, frequent episodes of acute rejection are known to be highly associated with the development of this irreversible process [4]. As the occurrence of acute rejection episodes often is the most predictive factor for the later development of chronic rejection in adults [5] and children [6], many clinicians advocate strategies to detect and ablate acute rejection episodes as early as possible. Although histologic evaluation from renal biopsy is generally accepted as the "gold standard" for diagnosing graft rejection, the biopsy procedure exposes the patient to the risk of possible bleeding, kidney rupture, infection, and arterial venous fistula, potentially even causing the loss of the graft [2, 7]. Thus, there is an urgent need to develop reliable organ- and/or cell-specific, noninvasive techniques for in vivo detection of organ rejection.

T-cell recognition of allo-antigen releases signals that trigger T-cell activation, and the subsequent infiltration of activated $CD4^+$ and $CD8^+$ T cells, macrophages, and natural killer cells into the graft are key events of acute allograft rejection [8]. Although T-cell–rich interstitial nephritis is a hallmark of acute allograft rejection, macrophages and their associated products, cytokines, may

Key words: immune cells, T cell, ultrasmall superparamagnetic iron oxide, kidney transplantation, acute rejection.

Received for publication December 6, 1999
and in revised form February 25, 2000
Accepted for publication March 15, 2000

influence initial and late changes and may be more important in the process than hitherto appreciated [9–11].

Since T cells and macrophages accumulate at the site of inflammation, thus leading to graft rejection, we are developing noninvasive methods to monitor the presence and accumulation of these immune cells in vivo by magnetic resonance imaging (MRI) techniques. The aim of the present study was to investigate the feasibility of using MRI to detect the accumulation of immune cells containing ingested ultrasmall superparamagnetic iron oxide (USPIO; it should be noted that in our previous publications [12–14], we used the terminology "SPIO" for particles of size similar to those used in the present study, namely approximately 30 nm. However, in this article, we refer to them as "USPIO," consistent with the terminology used by other groups [15–20] to differentiate them from the larger iron oxide particles, which exhibit different biodistribution properties.) particles in vivo in rejecting transplanted kidney of a rat, with the view of developing a new noninvasive way to detect early stages of graft rejection. Superparamagnetic iron oxide (SPIO) and USPIO particles reduce the MR signal intensity of water because of the magnetic susceptibility effect produced by iron and are excellent MR contrast agents [15]. Large SPIO particles (for example, AMI-25 with mean diameter ≈150 nm), which have been used as MRI contrast agents for detecting liver cancer and spleen tumors [16, 17], accumulate in cells of the mononuclear phagocytic system (MPS) of liver and spleen and are cleared from the blood within minutes. Smaller SPIO particles (for example, AMI-227, USPIO with mean diameter ≈20 nm) have an intravascular distribution, migrate very slowly across the capillary endothelium, have a longer half-life of about two hours in blood [18–20], are not immediately recognized by the MPS of liver and spleen, and are amenable to uptake by macrophages in more widespread areas of tissue. They can be eliminated without glomerular filtration by the organs of the MPS [19]. The slow elimination of these small particles allows the observation of signal modification in the vascular space.

There are two potential approaches for labeling immune cells that accumulate in the graft rejection process. First, the cells can be labeled ex vivo by a suitable MRI contrast agent, such as dextran-coated USPIO particles [12], and then the labeled cells can be infused into an animal as we have done to track the migration of USPIO-labeled T cells to the site of an inflammation created by the injection of calcium ionophore (A23187) into a rat testicle [13]. Second, USPIO particles can be infused intravenously into an animal in the hope of detecting the accumulation of USPIO-containing immune cells at the rejecting graft. This second approach is based on the recent finding of the detection of macrophage infiltration of the kidney by MRI after injection of USPIO particles in a rat model of experimental nephropathy caused by intravenous injection of puromycin aminonucleoside [21]. In the present study, detection of immune cell accumulation was tested in rats with transplanted kidneys by measuring the MRI signal intensity of the transplanted kidneys following infusion of USPIO particles by staining with immunohistologic markers and by staining with iron markers.

METHODS

In vitro MR and TEM assessment of the uptake of USPIO particles by macrophages

Uptake of USPIO particles by macrophages was assessed in vitro by exposing a macrophage cell population to USPIO particles, followed by MRI and transmission electron microscopy (TEM) investigations. Macrophages were isolated from the spleens of BN rats according to published methods [22] and were cultured in reconstituted RPMI 1640 culture medium (GIBCO, Grand Island, NY, USA) under 5% CO_2 at 37°C. The cells were then incubated with USPIO (2 mg Fe/10 $\times$ 10^6 cells) for 20 hours and recovered with three washes of phosphate-buffered saline (PBS).

High-resolution gradient-echo MR images of labeled and unlabeled macrophage cell phantoms (containing 2 $\times$ 10^6 and 0.5 $\times$ 10^6 cells/mL) were obtained using a 7-T, 15 cm horizontal bore Bruker AVANCE DRX MR instrument equipped with a 4.3 cm microimaging gradient set. Acquisition parameters were TR/TE = 1000/30 ms; flip angle = 45°; matrix size = 256 $\times$ 256, giving an in-plane resolution of 50 $\times$ 50 μm; slice thickness = 100 μm; acquisition bandwidth = 25 kHz; number of averages = 4; and scan time = 17 minutes.

Transmission electron microscopy was performed to characterize further the location of USPIO particles in the macrophages. The MRI and TEM studies on macrophages followed the procedures described earlier for the characterization of USPIO-labeled T cells [14].

Animals

Inbred DA ($RT1^a$) and BN ($RT1^n$) male rats (200 to 250 g) were purchased from Harlan-Sprague Dawley (Indianapolis, IN, USA) and were housed in the animal facility of the Pittsburgh NMR Center for Biomedical Research (Carnegie Mellon University, Pittsburgh, PA, USA). Animal care and experimentation were in compliance with the principles described in the *Principles of Laboratory Animal Care and Guide for the Use of Laboratory Animals*, published by the National Institutes of Health (NIH Publication no. 96-03, revised 1996). The present study was approved by the Institutional Animal Care and Use Committee of Carnegie Mellon University.

Renal transplantation

Transplantation was performed on male rats approximately 8 to 10 weeks old, weighing 250 to 300 g. BN rats

were used as recipients throughout and as donors for syngeneic transplantation (isografts), while DA rats served as donors for allogeneic transplantation (allografts). The animals were anesthetized by inhalation of methoxyflurane (Mallinckrodt Veterinary, Mundelein, IL, USA). The left nephrectomy of the recipient was performed before the left kidney transplantation. The graft (the donor left kidney) was flushed with University of Wisconsin solution (DuPont Pharma, Wilmington, DE, USA) containing heparin and then stored in the same solution at 4°C. The ischemia time was 15 to 20 minutes. Following the microsurgical technique of Lee, the donor renal artery and vein were anastomosed end to side to the recipient abdominal aorta and inferior vena cava with 10-0 sutures (Prolene; ETHICON, Somerville, NJ, USA) [23]. The ureter of the recipient was anastomosed end to end with the donor's ureter by 11-0 sutures (Ethilon; ETHICON) using four stitches. The right kidney was kept intact as an internal control for each individual rat transplantation. Thirty-four transplantations were performed for our studies in six groups. Transplants were examined by MRI before, immediately after, and one day after infusion of USPIO particles. Syngeneic transplants were infused with USPIO particles at postoperative day (POD) 4 ($N = 6$). Allogeneic transplants were infused at POD 2 ($N = 3$), POD 4 ($N = 12$), and POD 6 ($N = 3$), and allogeneic transplants were infused with a triple immunosuppressive treatment at POD 4 ($N = 5$). The triple immunosuppressive treatment consisted of daily subcutaneous injections of methylprednisolone (2 mg/kg; Pharmacia, Kalamazoo, MI, USA), rapamycin (1 mg/kg; Sigma, St. Louis, MO, USA), and cyclosporine A (CsA, 5 mg/kg; Sandoz, East Hanover, NJ, USA) on POD 1 through POD 4. One group of allograft recipients ($N = 5$) was sacrificed at POD 1 without USPIO infusion to serve as a baseline for evaluating the cellular kinetics.

Preparation and infusion of USPIO particles

A stock suspension of dextran-coated USPIO particles was synthesized in our laboratory according to Palmacci and Josephson [24] with slight modifications. The initial iron content in the particle suspension was determined for all samples using a spectrophotometric method [25]. Iron-core size, mean diameter of whole particles, and MR relaxation measurements of USPIO particles were carried out as described in Dodd et al [14]. Iron-core size measured by TEM was found to be in the range 4.0 to 7.5 nm. Mean diameter of whole particles measured by laser light scattering was 29 ± 3 nm. The MR relaxivities, R_1 (spin-lattice relaxation rate constant, $1/T_1$, per mole of Fe in USPIO) and R_2 (spin-spin relaxation rate constant, $1/T_2$, per mole of Fe in USPIO), at 4.7 T were 3.8×10^4 and 9.1×10^4 mol/L^{-1} s^{-1}, respectively.

Prior to infusion of USPIO particles for in vivo studies, a portion of the stock suspension was dialyzed in PBS, filter sterilized, and assayed for iron content [25]. The solution was diluted with PBS to a concentration of 9 μmol Fe/mL, and 0.5 mL of the suspension was injected intravenously for each study.

In vivo MRI studies of renal transplantation

In vivo studies of the effect of USPIO particle infusion on transplanted kidneys were performed on a 4.7-T, 40 cm horizontal bore Bruker AVANCE DRX MR instrument. The rats were under general anesthesia with endotracheal intubation (O_2 70%, N_2O 30%, and 1.5% isoflurane) during the MR experiments. A 20 cm PE50 catheter was inserted into the left jugular vein for the infusion of USPIO particles. Coronal MR images of bilateral kidneys were obtained before, immediately after, and 22 to 24 hours following infusion of USPIO particles. Gradient-echo images were triggered to respiratory motion with: TR/TE = 1000/12 ms; flip angle = Ernst angle; slice thickness = 1 mm; 15 contiguous slices; field of view = 7.0 cm; data matrix size = 256 × 130 (zero-filled to 256 × 256); two averages; and scan time = 4.3 minutes. Field homogeneity was optimized by shimming on a slice centered on both kidneys.

The average changes of MR signal intensity were measured in two different compartments, cortex and medulla, both in transplanted and native kidneys. Regions of interests (ROIs) for cortex and medulla were traced by hand (using the Bruker image processing software) on the center slice of each kidney (or as close as possible). Regions were defined on the MR images acquired immediately after the infusion of the USPIO particles, which showed the best corticomedullary differentiation; these ROIs were also used to analyze the preinfusion images. ROIs for the images acquired one day later were drawn to be as close as possible to the initial ROIs. A typical ROI drawn for the cortex was comprised of 150 pixels (volume of approximately 11 mm^3) and for the medulla of 500 to 600 pixels (volume of approximately 37 to 45 mm^3). MR signal intensity was normalized to that of muscle of the same rat, as the muscle tissue was known not to readily take up iron [21]. The signal intensity reduction in each animal was calculated according to:

$$100 \cdot (I_{pre} - I_{post})/I_{pre} \qquad \text{(Eq. 1)}$$

where I_{pre} is the signal intensity before USPIO infusion, and I_{post} is the signal intensity after USPIO infusion, with both first normalized to the muscle signal intensity.

Histology, immunohistochemistry, and iron staining for USPIO detection

Rats were sacrificed for histologic evaluations at one day after USPIO infusion following the MRI studies. Before each animal was sacrificed, 0.5 mL of blood was sampled for analysis of serum creatinine content. The harvested graft and native kidneys were fixed in 3.7%

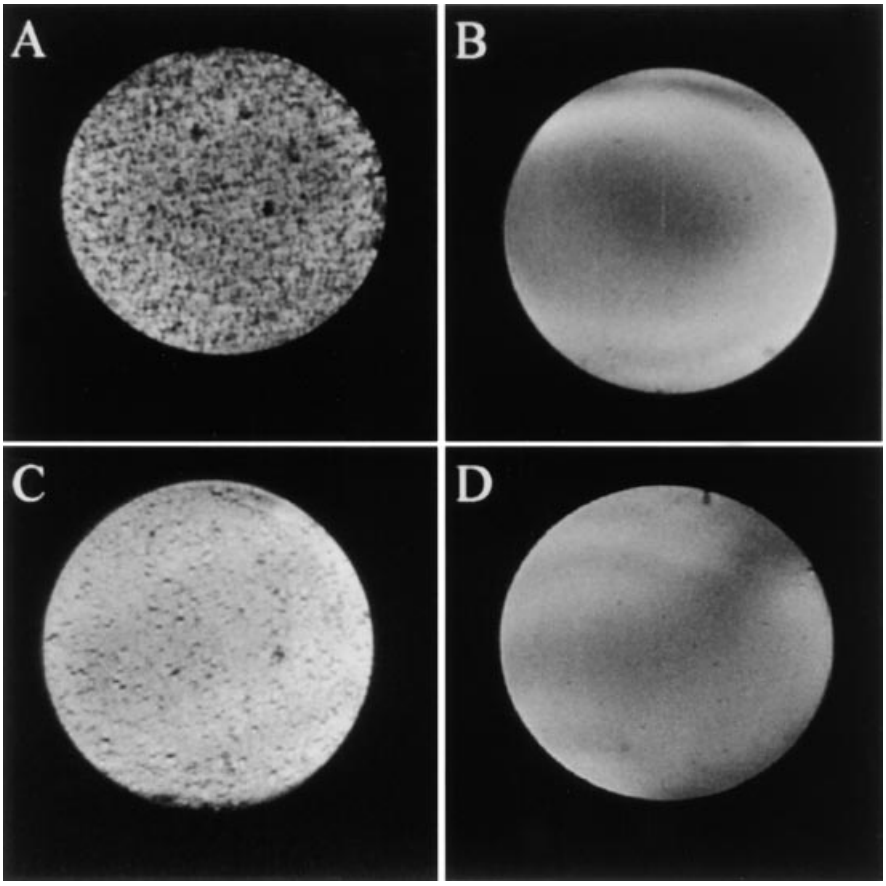

Fig. 1. Gradient-echo magnetic resonance (MR) images showing ultrasmall superparamagnetic iron oxide (USPIO)-labeled (*A* and *C*) and unlabeled (*B* and *D*) macrophage samples in vitro. Cell concentrations were as follows: (A and B), 2.0×10^6 cells/mL and (C and D), 0.5×10^6 cells/mL. Bulk samples for these high-resolution MRI studies were prepared in 1 mL plastic syringes by suspending labeled or unlabeled macrophages in 5% gelatin. The dark spots in A and C appear to represent single USPIO-labeled macrophages. The slow varying shadow seen in (B and D) are believed to be due to bulk field inhomogeneity brought about by imperfect shimming of the magnet.

formaldehyde and embedded in paraffin and then were longitudinally cut into sections of 5 μm thickness. Sections from such samples were stained with hematoxylin and eosin (HE) and Perl's Prussian blue (for visualizing iron particles), respectively. One piece of fresh samples from each animal was fixed in 2% glutaraldehyde buffered with PBS for TEM studies.

Sections from the third piece were snap frozen in OCT (Tissue-Tek; Miles Inc., Elkhart, IN, USA) in cryomolds and embedding rings and were stored under liquid nitrogen. Cryostat sections were cut at −22°C and thaw mounted on glass slides. The sections were air dried, fixed in cold acetone, and stained individually with an appropriate dilution of primary mouse anti-rat monoclonal antibodies against CD4 (T-helper cells), CD8 (cytotoxic T cells), and ED1 (macrophages) in PBS, pH 7.4, with 1% bovine serum albumin for one hour in a humidified chamber. ED1 (Serotec, Raleigh, NC, USA) recognizes a CD68-like antigen in most cells of the monocyte/macrophage system, while CD4 and CD8 (Serotec) recognize T-cell surface antigens. The sections were then interacted with rabbit anti-mouse IgG by 3-amino-9-ethylcarbazole (AEC; red color in CD8) or by peroxidase-rabbit antiperoxidase (PAP; brown color in CD4 and ED1) based on the avidin-biotin-peroxidase complex (ABC) method [26]. Sections were counterstained with Mayer's hematoxylin before permanent mounting. Control sections were incubated with the same solution without primary antibodies. Cellular infiltration in the renal cortex and medulla of each rat was expressed as the number of cells per field of view (c/FV) at a magnification of ×400; at least 10 fields of view were evaluated for each section.

Statistical analysis

The data were expressed as mean ± SD. The Student's *t*-test was used for comparison of results between two groups. For comparisons involving more than two groups, analysis of variance and the Student–Newman–Kuels test were applied. P values ≤ 0.05 were considered significant.

RESULTS

In vitro MR and TEM studies of USPIO particles in macrophages

Gradient-echo MR images of USPIO-labeled and -unlabeled macrophages in 5% gelatin are shown in Figure 1. Figure 1 A and B show USPIO-labeled and -unlabeled

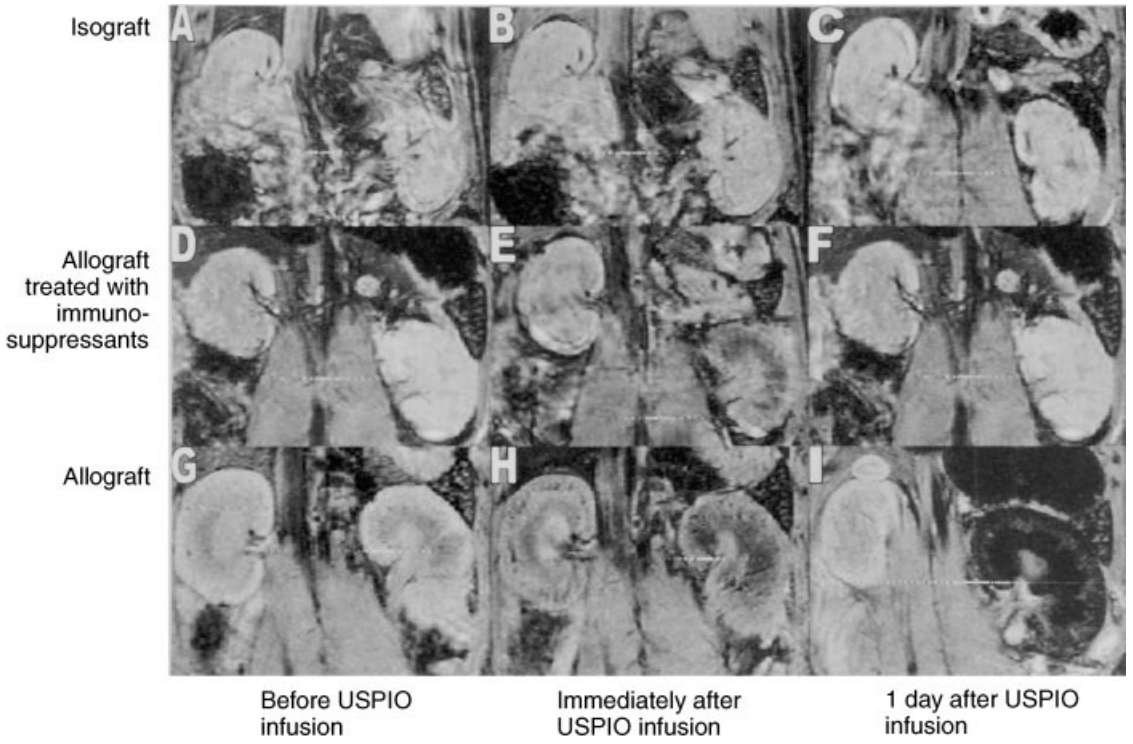

Fig. 2. Gradient-echo MR images showing the effect of USPIO infusion. (*A–C*) Images from an isograft study immediately before (A) and immediately after (B) USPIO infusion at POD 4, as well as one day following USPIO infusion (C) at POD 5. Images in (*D–F*) are from an allograft experiment with a triple immunosuppressant treatment at corresponding time points and (*G–I*) are from an allograft study without immunosuppressant treatment. In these panels, the transplanted kidneys appear on the right, and the native kidneys appear on the left. The allograft study without the immunosuppressant treatment (I) shows a decrease of the MR signal intensity within the transplant at one day after USPIO infusion. This decrease in MR signal intensity is believed to be due to an accumulation of macrophages containing USPIO particles in the rejecting transplanted kidney.

samples, respectively, with a concentration of 2×10^6 macrophages/mL. Figure 1 C and D show USPIO-labeled and -unlabeled samples, respectively, with a concentration of 0.5×10^6 macrophages/mL. Based on our USPIO-labeled T-cell results [14], we believe that each dark spot in the labeled samples (Fig. 1 A, C) represents a single USPIO-labeled macrophage. The density of these dark spots appears to be dependent on the concentration of macrophages. Measurements by TEM revealed that the labeling efficiency of macrophages by USPIO particles in vitro is approximately 80%. This is much higher than the labeling efficiency previously measured for T cells (20%) [14]. The labeling efficiency of USPIO particles for both macrophages and T cells in vivo is not assessed in this study.

In vivo MRI studies of renal transplantation

The effect of USPIO particle infusion at POD 4 on MRI of transplanted kidneys is shown in Figure 2 for single studies within each of the three experimental groups: isograft; allograft with a triple immunosuppressant treatment; and allograft without immunosuppressants. The transplanted kidneys appear on the right side of the figures, with native kidneys on the left side. MR images are shown from an isograft study immediately before (Fig. 1A), and immediately after (Fig. 1B) USPIO infusion at POD 4, and one day after USPIO infusion (Fig. 1C). Images at corresponding time points are shown in Figure 2 D–F for allogeneic transplanted rats treated with immunosuppressants and in Figure 2 G–I for allografts without immunosuppressant treatment. The allograft without immunosuppressant treatment clearly shows an effect in the transplanted kidney at one day following USPIO infusion, that is, an almost complete darkening of the inner medulla and substantial signal decreases in the cortex and outer medulla (Fig. 2I). This MR signal reduction is believed to be due to the presence of USPIO particles in macrophages present in the rejecting kidney. Immediately after the infusion, some darkening can be seen in both native and transplanted kidneys of most samples studied because of the presence of the USPIO particles in the vasculature.

Table 1 summarizes the MR signal intensity reduction from five groups of renal transplanted rats, that is, isograft group at POD 5 ($N = 5$), allograft group with a triple immunosuppressive treatment at POD 5 ($N = 5$),

Table 1. Magnetic resonance imaging (MRI) signal intensity reduction of transplanted kidneys

Group	% change of MRI signal intensity	
	Cortex	Medulla
Isograft ($N = 5$), POD 5	-3.7 ± 10.4	-1.6 ± 4.5
Allograft treated with immunosuppressants ($N = 5$), POD 5	-1.9 ± 15.3	0.8 ± 9.3
Allograft[a] ($N = 11$), POD 5	44.4 ± 33.5	39.1 ± 37.3
Allograft[b] ($N = 3$), POD 3	-6.2 ± 2.8	-18.3 ± 31.9
Allograft[b] ($N = 3$), POD 7	-8.6 ± 19.8	-25.9 ± 44.9

Data are mean ± SD. Negative values represent an increase in the MRI signal intensity following infusion of USPIO particles. Details are in the text.

[a] Allografts without immunosuppressive treatment at postoperative day (POD) 5 showed significant change ($P < 0.05$) before and 24 hours after infusion of USPIO particles (results not shown)

[b] One study each for the POD 3 and POD 7 groups showed low MR signal within the transplanted kidney before infusion of USPIO particles

and allograft groups without immunosuppressive treatment at POD 3 ($N = 3$), POD 5 ($N = 11$), and POD 7 ($N = 3$). The negative values in Table 1 represent an increase in MRI signal intensity following infusion of USPIO particles. Only the allograft group without immunosuppressive treatment at POD 5 exhibited substantial MR signal intensity reduction in both the cortex and medulla. In the allograft group without immunosuppressive treatment at POD 5, MR signal intensity did not decrease in the cortex nor in the medulla in three studies nor in the medulla in two studies, resulting in a high standard deviation (SD) of that group. Only in the case of allograft group without immunosuppressive treatment was there a significant difference ($P < 0.05$) between pre- and postinfusion of USPIO means (results not shown). One syngeneic sample that showed abdominal duct leakage leading to severe infection and one allogeneic sample without immunosuppressive treatment that showed severe peritonitis caused by abdominal lymphatic duct leakage were excluded from numerical analysis in Table 1; these two studies showed a reduction of MR signal intensity in both transplanted and native kidneys.

Histological studies

The blood chemistry showed that there was no significant increase of serum creatinine levels in any of the groups studied (results not shown). The low creatinine levels are attributable to the existence of the contralateral native kidney [27].

In allografts without immunosuppression, several histologic changes were noted at POD 3 after engraftment, that is, a mild epithelial edema of tubules and a mild interstitial mononuclear cell infiltration. By POD 5, the allograft kidneys were enlarged, and the presence of acute rejection was confirmed. These morphological changes are characteristic of acute rejection of type A, namely a significant increase of host mononuclear cell infiltration in the interstitium, particularly in or around glomeruli, and in vessels and perivascular areas (intimal arteritis), and foci of severe tubulitis [28]. By POD 7, vessel walls were disrupted, and tubular cells were becoming edematous and necrotic. Both allografts with a triple immunosuppressive treatment and isografts showed minimal histologic changes at five days post-transplantation, with no apparent changes in the gross appearance compared with that of native kidneys (results not shown).

Immunohistochemistry

Stained cryosections of allograft kidneys without immunosuppressive treatment at POD 5 are shown in Figure 3. $CD4^+$ and $CD8^+$ T cells have extensively infiltrated the glomerular capillary lumina, accompanied by swelling of endothelial cells in the perivascular region and interstitium. A large quantity of $CD4^+$ and $CD8^+$ T cells has infiltrated both the cortex (Fig. 3 A, C) and the medulla (Fig. 3 B, D). There are densely infiltrated areas of $CD4^+$ and $CD8^+$ T cells in each section, mostly surrounding the vessels and glomeruli or tubules of the medulla. ED1 staining shows that a large resident population of $ED1^+$ macrophages is present in the tubulointerstitium and around or in the glomeruli of allograft kidneys without immunosuppressive treatment (Fig. 3 E, F). The infiltration became more prominent as the severity of kidney rejection increased during the acute rejection process. Very few $ED1^+$ macrophages and $CD4^+$ and $CD8^+$ T cells were found in isografts, allografts with immunosuppressive treatment, or native kidneys (results not shown).

Macrophages and T cells of both cortex and medulla were detected immunochemically in cryostat sections in each allograft without immunosuppressive treatment. Graphs of the quantitative results are shown in Figure 4. At days 3 and 5 post-transplantation, $CD4^+$ and $CD8^+$ populations and ED1 monocytes/macrophages increased; this increase reached very substantial levels at POD 5, decreasing thereafter (Fig. 4).

Table 2 summarizes our immunohistologic results at POD 5 of kidney allografts, allografts with a triple immunosuppressive treatment, and isografts. Immune cell infiltration was dramatic in the allograft group without immunosuppressive treatment at five days post-transplantation. Only mild immune cell infiltration occurred in the allograft group with immunosuppressive treatment, while minimal infiltration was observed in the isograft group.

There was dense staining of $CD4^+$ and $CD8^+$ T cells aggregated in adjacent arteries (white pulp) in the spleen of allograft animals (results not shown). In contrast, there was minimal dense staining of $ED1^+$ macrophages in the parenchyma (red pulp) of the spleen (results not shown). The discrepancy between T-cell and macrophage locations may reflect the activity of recruit-acti-

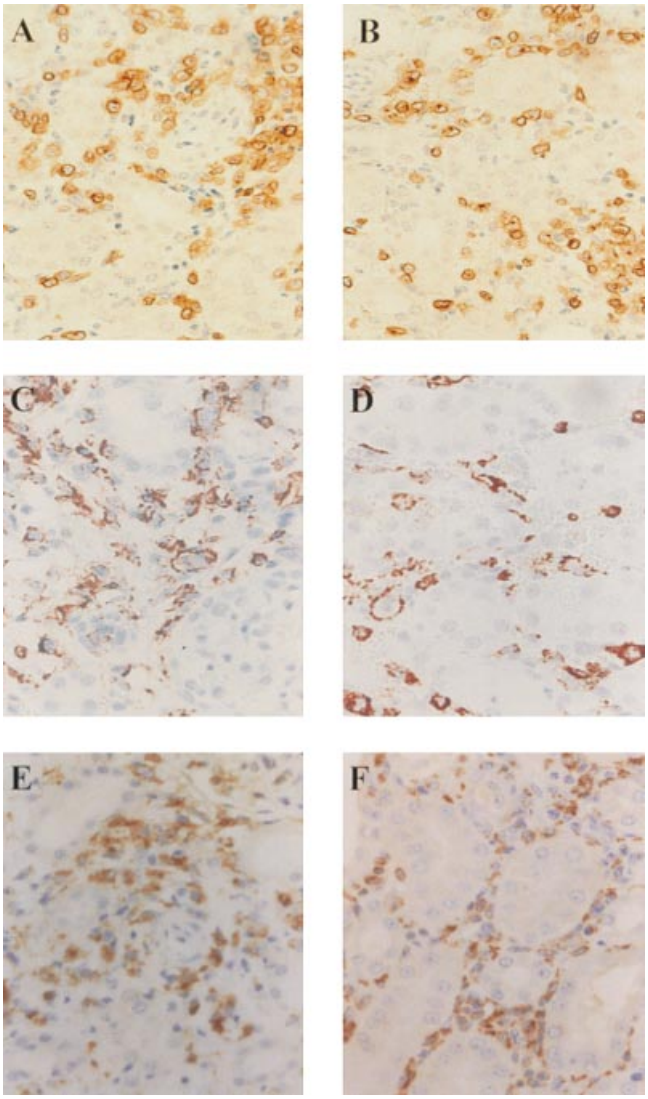

Fig. 3. Optical microscopy showing immunohistochemical detection of CD4$^+$ and CD8$^+$ T-cell and ED1$^+$ macrophage infiltration at postoperative day (POD) 5 in allograft kidneys without immunosuppressive treatment. Cryosections were stained with monoclonal antibodies to CD4 and CD8 T cells and ED1 macrophages, and then the sections were reacted with rabbit or goat anti-mouse IgG by AEC (red color in CD8) or by PAP (brown color in CD4 and ED1). (*A* and *B*) CD4$^+$ T cells. (*C* and *D*) CD8$^+$ T cells. (*E* and *F*) ED1$^+$ macrophages. (A, C, and E) are cortex and (B, D, and F) are medulla. Magnification ×400.

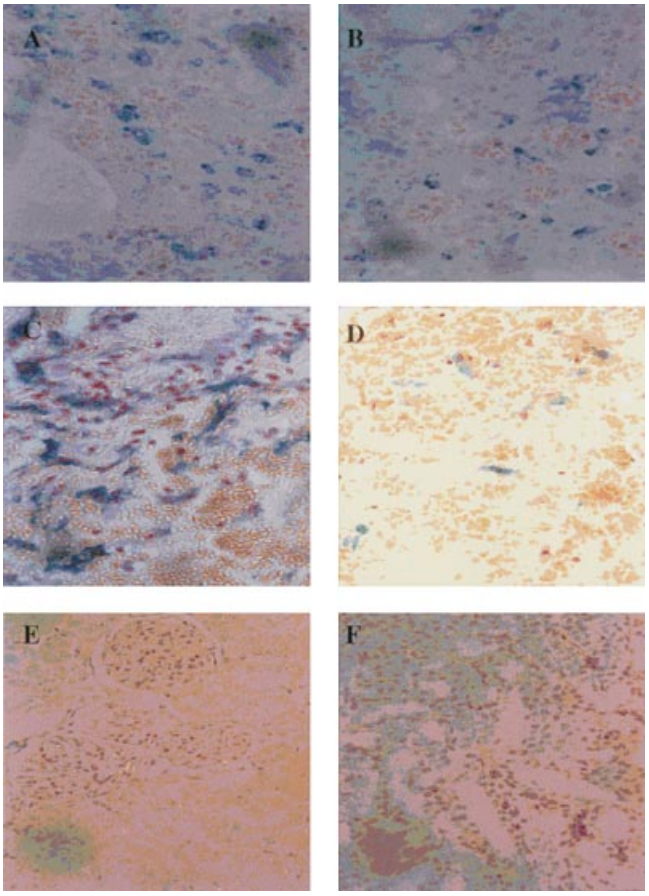

Fig. 5. Optical microscopy of graft kidneys stained with Perl's Prussian blue at POD 5: Allograft kidneys without immunosuppressive treatment (*A–D*) and isograft kidneys (*E*) and (*F*). (A, C, and E) Cortex and (B, D, F) medulla. There were large numbers of dense core plaques in (A) surrounding the glomeruli or renal tubular structure. Amorphous plaques and empty cores were found in the perivascular, renal encapsulate distribution (C) and in the blood vessels (D) of allograft kidneys. No iron plaques were found in either cortex (E) or medulla (F) of isograft kidneys. Magnification ×200.

vated macrophages in spleen, which are responsible for the intake and destruction of particulate antigens.

Iron staining for USPIO detection

After staining with Perl's Prussian blue, iron deposits were observed in macrophages both in the cortex (around glomeruli, tubules, and vessels) and the medulla (in interstitium) at POD 5 in allografts without immunosuppressive treatment (Fig. 5 A–D). In each sample of this group, iron was visibly stained in the outer medulla adjacent to the cortex. Round macrophages, typically with high concentrations of iron, were present in 7 out of 10 allograft recipients. A high concentration of iron-containing macrophages was also identified in spleen parenchyma of all groups at three, five, and seven PODs in this study. The iron plaques in macrophages could be categorized as one of three types: dense core plaques (Fig. 5A), diffuse amorphous plaques (Fig. 5 C, D), or empty core plaques (Fig. 5 C, D). The dense core plaques often had a halo of stain surrounding them with an unstained area between the dense core and the halo. Sometimes, there were several dense core plaques surrounding the nucleus in one macrophage. Small, dense iron plaques distributed mostly in the cortex (near vessels or in glomeruli; Fig. 5A). Amorphous plaques were consistently stained throughout their width; these plaques were often distributed near or in blood vessels in an allograft kidney. The empty core plaques had a center that was unstained. In isograft

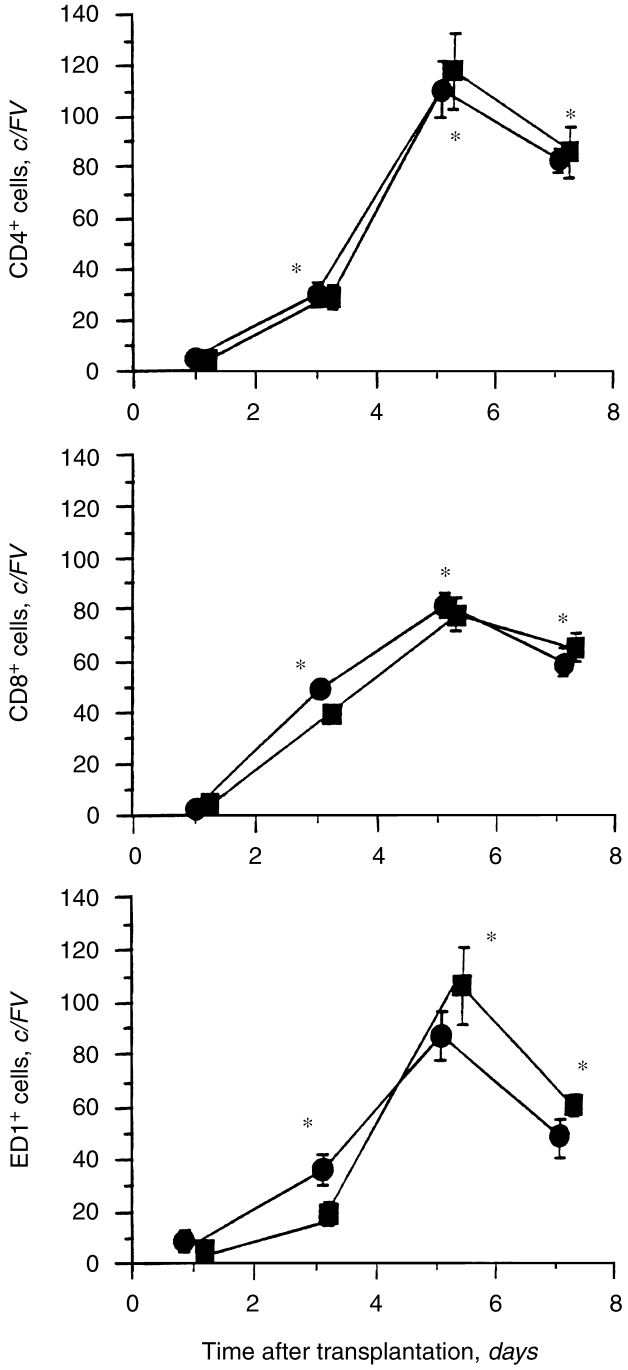

Fig. 4. Quantitation of CD4+ and CD8+ T-cell and ED1+ macrophage infiltration in allograft kidneys without immunosuppressive treatment. Cell counts were performed under an optical microscope at a magnification of ×400 at POD 1 ($N = 5$), POD 3 ($N = 3$), POD 5 ($N = 11$), and POD 7 ($N = 3$). Minor offsets (<0.5 day) along the POD axis between groups are for illustrative purposes only and do not represent a real shift in time. Data are expressed as mean ± SE. Symbols are: (●) cortex; (■) medulla; *$P < 0.05$ by Student's t-test for days 3, 5, and 7 versus day 1 for cortex and medulla. The abbreviation c/FV is the number of cells per field of view.

kidneys, Prussian blue staining was not observed in the cortex (Fig. 5E) or in the medulla (Fig. 5F), nor were iron plaques observed in native kidneys or in allograft kidneys with immunosuppressive treatment. The distribution of iron plaques as seen by Perl's Prussian blue staining was well correlated with the distribution of ED1+ macrophages in allograft kidneys without immunosuppressive treatment at POD 5 (results not shown). However, there was no observable evidence of iron particles in the T cells of the allograft kidneys without immunosuppressive treatment, presumably because of the much smaller number of T cells containing USPIO particles. Our previous results indicated that about 20% of T cells took up USPIO particles under cell culture conditions [14], whereas about 80% of macrophages ingested the USPIO particles in the present study.

Ultrastructure of the USPIO-lysosomes contained in the kidney

Figure 6 shows TEM detection of iron particles within the lysosomes of a macrophage from an allograft kidney. A number of granules composed of iron particles were observed in lysosomes. Many granules form one vacuole unit, which we believe to be the plaque seen in optical microscopy after Prussian blue staining. No free iron particles were observed in the tubular cells and interstitium. There was no evidence of iron particles in either the native kidneys, isograft kidneys, or the allograft kidneys with triple immunosuppressive treatment. There were numerous dense iron vacuoles contained in the macrophages of the spleen in each animal.

DISCUSSION

The most important finding of this work is that intravenous infusion of USPIO particles caused a significant decrease in the MR signal intensity of allogeneic transplanted kidneys in rats compared with those of control nontransplanted kidneys. Immediately after a bolus injection of USPIO particles containing 4.5 μmol iron, signal intensity reduction was usually detectable in MR images in both native and transplanted kidneys and in liver, spleen, and large blood vessels because of the presence of USPIO particles in the vascular system. At one day following USPIO infusion on POD 4, the MR signal intensity of the native and isograft kidneys and allograft kidneys with a triple drug immunosuppressive treatment was restored to the level of preinfusion. In contrast, after transplantation of allograft kidneys without immunosuppressive treatment in our rat model (DABN), MRI signal intensity of the transplanted kidney in the allograft group was decreased one day following the initial infusion of USPIO particles on POD 4 (Table 1). Our results have confirmed that acute rejection can be effectively inhibited in kidney allografts administered with a triple-drug

Table 2. Immunohistology at postoperative day (POD) 5 of kidney allografts, allografts with a triple immunosuppressive treatment, and isografts

		ED1$^+$ cells (c/FV)		CD4$^+$ cells (c/FV)		CD8$^+$ cells (c/FV)	
Groups	*N*	Cortex	Medulla	Cortex	Medulla	Cortex	Medulla
Allografts	11	84.8 ± 9.1	106.7 ± 14.1	109.8 ± 9.4	116.5 ± 10.7	80.4 ± 10.6	76.3 ± 15.2
Allografts[a]	5	7.8 ± 1.7[b]	9.6 ± 1.1[b]	12.6 ± 2.7[b]	14.3 ± 2.1[b]	19.5 ± 2.5[b]	20.8 ± 2.5[b]
Isografts	6	0.3 ± 0.5[b]	0.2 ± 0.4[b]	1.2 ± 0.9[b]	2.7 ± 1.6[b]	0.2 ± 0.4[b]	0.1 ± 0.8[b]

[a] Allografts with a triple immunosuppressive treatment (see text for details)
[b] $P < 0.001$, allografts treated with triple immunosuppressive treatment vs. allografts, and isografts vs. allografts

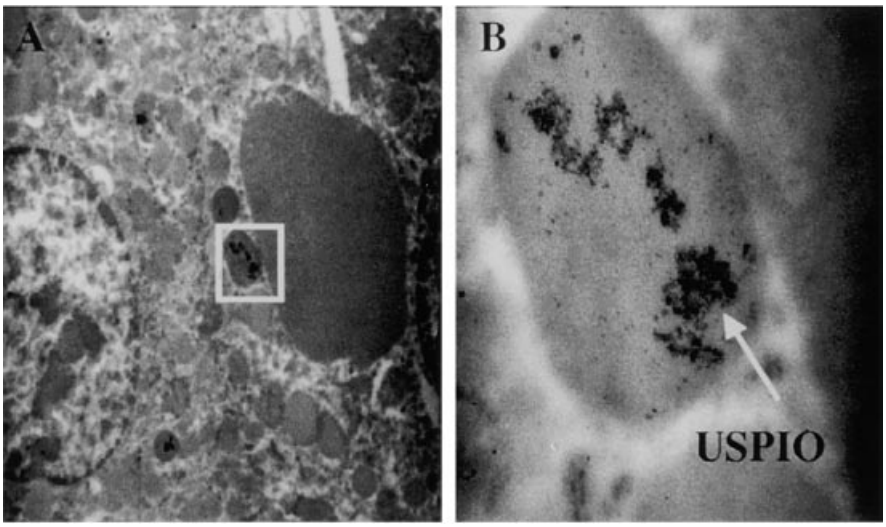

Fig. 6. Transmission electron microscopy (TEM) results showing ultrastructural morphology of a macrophage in an allograft kidney without immunosuppressive treatment at POD 5. (*A*) USPIO particles were contained within a vacuole (in square) in a macrophage near the outer medulla, with several particles accumulating within one vacuole. (*B*) The vacuole itself [expansion of area within square of (A) was a lysosome containing many dense granules of USPIO particles, arrow head]. Magnification ×9400 in A; ×70,700 in B.

immunosuppressive treatment [29]. This study shows a consistent progression of infiltration of ED1$^+$ macrophages and CD4$^+$ and CD8$^+$ T-cells that peaks at POD 5 after transplantation (Fig. 4), as well as MRI signal intensity reduction (Table 1) in transplanted kidneys of the allograft group without immunosuppressive treatment. Prussian blue staining shows the existence of numerous iron plaques in the cortex and medulla of the untreated allograft (Fig. 5). We attribute each plaque to a large vacuole phagocytosed by macrophages, which then infiltrate the interstitium of the allograft kidney. The presence of USPIO-containing vacuoles in macrophages is believed to cause the decrease in the MR image intensity as shown in Figure 2I in the cortex and medulla of untreated allograft kidneys at POD 5.

A potential advantage of USPIO particles over macromolecular MRI contrast agents is that intracellular degradation of USPIO particles occurs in tubular lysosomes and iron degradation products are incorporated into the normal pathway. Prior studies have shown no cytotoxic effect of USPIO in cell culture and in the human body [12, 13, 16–19, 30–32]. USPIO particles can act as an MRI blood-pool contrast agent, which can be used to mark the vascular compartment within the first few hours after infusion of USPIO particles. It is possible to evaluate the functional changes of the kidney based on the USPIO vascular kinetics in this early period. However, USPIO particles in the normal vasculature are eliminated quite slowly, as their half-life in the rat is about two hours [15, 17–20].

We postulate that the macrophages that infiltrate the allograft kidneys may have several different origins. One major source probably is blood monocytes, since the renal vessels contain a large proportion of monocytes saturated with USPIO particles. In the group of allograft recipients at 7 days post-transplantation and in some cases at POD 5, the allograft kidneys experienced severe rejection and were greatly enlarged without MR signal loss. It was shown in our recent study that the renal cortical perfusion rate in allogeneic transplanted kidneys at the peak of acute rejection is greatly reduced compared with that in syngeneic kidneys [27]. The reduced blood flow may be insufficient to supply enough blood macrophages and lymphocytes carrying USPIO particles to the graft, which could account for the substantially lower reduction in MR signal intensity observed at those time points. In our DA→BN rat model, severe acute rejection begins around POD 5, but variations in the initiation of rejection could occur. Although the role of local proliferation of immune cells in augmentation of

allograft injury is still a controversial issue, a number of recent studies have shown that local proliferation of inflammatory macrophages plays an important role in macrophage accumulation and renal injury in immunologically induced models of severe renal injury, such as acute allograft rejection [33, 34]. In the study of Yang et al, there was a highly significant correlation between local macrophage proliferation and macrophage-mediated progressive renal injury, irrespective of the nature of the initial renal injury, thus providing a second possible origin of macrophages [34]. However, locally proliferated macrophages distributed in the interstitium of the allograft kidney may lack access to USPIO particles, which exist in the vascular space. A third possible origin of macrophages giving rise to the pathogenesis of acute rejection may be proliferation from kidney mesangial cells of glomeruli [35, 36].

The detection of macrophage infiltration would be useful in the follow-up of kidney transplantation to evaluate the functional changes in the grafts in patients with CsA nephrotoxicity, which can be differentially diagnosed only by biopsy at present. CsA nephropathy is arteriolopathy, not associated with macrophage and T-cell infiltration. CsA-associated arteriolopathy affects mostly afferent arterioles and terminal portions of interlobular arteries, which are characterized by localization of hyaline deposits within the medial layers of smooth muscle cells and at the outer surface of affected vessels [37]. MR signal loss occurs in tissue with a high population of macrophages after infusion of USPIO particles. Thus, the present MRI method might be able to differentially diagnose acute rejection with macrophage infiltration from CsA nephrotoxicity without macrophage infiltration. The limitation of this method is that it may be difficult to differentiate acute rejection from kidney infection or tubulopathy or ischemic injury. Further research is needed to develop and to understand imaging properties under different pathological conditions, with diagnosis based on both imaging results and pathological parameters (that is, symptoms, immunologic alterations).

In conclusion, our results show that an intravenous administration of USPIO particles into a transplanted animal appears to be a valuable tool for detecting the accumulation of macrophages at the site of graft rejection. The presence of the USPIO particles decreases the signal intensity of MR images at the site of allografts and thus provides a possible new, noninvasive means of detecting graft rejection not only in kidney, but also in other organs. Currently, our laboratory is carrying out similar studies in transplanted lungs and hearts in rats.

ACKNOWLEDGMENTS

This work is supported by research grants from the National Institutes of Health (R01RR-10962 and R01RR/AI-15187) and The Whitaker Foundation. The experiments were performed in the Pittsburgh NMR Center for Biomedical Research, which is supported by a grant (P41RR-03631) from the National Center for Research Resources as a National Institutes of Health-supported Resource Center. We wish to thank Ms. Maryann C. Butowicz for her excellent technical assistance, Mr. Joseph P. Suhan for carrying out the electron microscope measurements, the Transplant Histopathology Laboratory of the University of Pittsburgh Medical Center for analyzing our histologic data, and Dr. Charles A. Ettensohn for use of his optical microscope. We also thank Dr. Suzanne I. Ildstad, Dr. Christina L. Kaufman, Dr. Edwin K. Jackson, Dr. Pedro J. del Nido, Dr. Donald S. Williams, Dr. Shinichi Kanno, and Dr. E. Ann Pratt for helpful discussions.

Reprint requests to Dr. Chien Ho, Department of Biological Sciences, Carnegie Mellon University, 4400 Fifth Avenue, Pittsburgh, Pennsylvania 15213-2683, USA.
E-mail: chienho@andrew.cmu.edu

REFERENCES

1. Cho YW, Terasaki PI, Graver B: Fifteen year kidney graft survival, in *Clinical Transplant*, edited by Terasaki P, Los Angeles, UCLA Tissue Typing Laboratory, 1989, pp 325–331
2. Racusen LC, Solez K, Burdick JF (editors): *Kidney Transplant Rejection: Diagnosis and Treatment.* New York, Marcel Dekker, Inc., 1998
3. Johnson CP, Simmons RL, Sutherland DE, Canafax DM, Ascher NL, Payne WD, Flick BM, Najarian JS: A randomized trial comparing cyclosporine with anti-lymphoblast-globin-azathioprine for renal allograft recipients: Results at 2 1/2 to 6 years. *Transplantation* 45:380–385, 1988
4. Tullius SG, Tilney NL: Both alloantigen-dependent and independent factors influence chronic allograft rejection. *Transplantation* 59:313–318, 1995
5. Cecka JM: Outcome statistics of renal transplants with an emphasis on long-term survival. *Clin Transplant* 8(3 Pt 2):324–327, 1994
6. Tejani A, Stablein D, Alexander S, Fine R, Harmon W: Analysis of rejection outcome and implications: A report of the North American Pediatric Renal Transplant Cooperative Study. *Transplantation* 59:500–504, 1995
7. Foster MC, Morgan AG, Wenham PW, Rowe PA, Burden RP, Cotton RE, Blamey RW: The late results of renal transplantation and the importance of chronic rejection as a cause of graft loss. *Ann R Coll Surg Engl* 71:44–47, 1989
8. Nadasdy T, Krenacs T, Kalmar KN, Csajbok E, Bouda K, Ormos J: Importance of plasma cells in the infiltration of renal allografts: An immunohistological study. *Pathol Res Pract* 187:178–183, 1991
9. Paul LC, Grothman GT, Benediktsson H, Davidoff AL, Rozing J: Macrophage subpopulations in normal and transplanted heart and kidney tissue in the rat. *Transplantation* 53:157–162, 1992
10. Nagano H, Nadeau KC, Takada M, Kusaka M, Tilney NL: Sequential cellular and molecular kinetics in acutely rejecting allografts in rats. *Transplantation* 63:1101–1108, 1997
11. Takada M, Nadeau KC, Shaw GD, Marquette KA, Tilney NL: The cytokine-adhesion molecule cascade in ischemia/reperfusion injury of the rat kidney. *J Clin Invest* 99:2682–2690, 1997
12. Yeh TC, Zhang W, Ildstad ST, Ho C: Intracellular labeling of T-cells with superparamagnetic contrast agents. *Magn Reson Med* 30:617–625, 1993
13. Yeh TC, Zhang W, Ildstad ST, Ho C: In vivo dynamic MRI tracking of rat T-cells labeled with superparamagnetic iron-oxide particles. *Magn Reson Med* 33:200–208, 1995
14. Dodd SJ, Williams M, Suhan JP, Williams DS, Koretsky AP, Ho C: Detection of single mammalian cells by high-resolution magnetic resonance imaging. *Biophys J* 76:103–109, 1999
15. Chambon C, Clement O, Le Blanche A, Schouman-Claeys E, Frija G: Superparamagnetic iron oxides as positive MR contrast agents: *In vitro* and *in vivo* evidence. *Magn Reson Imaging* 11:509–519, 1993
16. Stark DD, Weissleder R, Elizondo G, Hahn PF, Saini S, Todd LE, Wittenberg J, Ferrucci JT: Superparamagnetic iron oxide: Clinical applications as a contrast agent for MR imaging of the liver. *Radiology* 168:297–301, 1988
17. Weissleder R, Hahn PF, Stark DD, Elizondo G, Saini S, Todd

LE, Wittenberg J, Ferrucci JT: Superparamagnetic iron oxide: Enhanced detection of focal splenic tumors with MR imaging. *Radiology* 169:399–403, 1988
18. Trillaud H, Degreze P, Combe C, Palussiere J, Chambon C, Grenier N: Evaluation of intrarenal distribution of ultrasmall superparamagnetic iron oxide particles by magnetic resonance imaging and modification by furosemide and water restriction. *Invest Radiol* 29:540–546, 1994
19. Majumdar S, Zoghbi SS, Gore JC: Pharmacokinetics of superparamagnetic iron-oxide MR contrast agents in the rat. *Invest Radiol* 25:771–777, 1990
20. Weissleder R, Elizondo G, Wittenberg J, Rabito CA, Bengele HH, Josephson L: Ultrasmall superparamagnetic iron oxide: Characterization of a new class of contrast agents for MR imaging. *Radiology* 175:489–493, 1990
21. Hauger O, Delalande C, Trillaud H, Deminiere C, Quesson B, Kahn H, Camber J, Combe C, Grenier N: MR imaging of intrarenal macrophage infiltration in an experimental model of nephrotic syndrome. *Magn Reson Med* 41:156–162, 1999
22. Coligan JE, Kruisbeek A, Margulies DH, Shevach EM, Struber W: *Current Protocols in Immunology.* New York, John Wiley and Sons, Inc., 1995
23. Lee S: An improved technique of renal transplantation in the rat. *Surgery* 61:771–775, 1967
24. Palmacci S, Josephson L: *Synthesis of Polysaccharide Covered Superparamagnetic Oxide Colloids, U.S. Patent, 5262176. Example 1.* November 16, 1993
25. Papisov MI, Bogdanov A Jr, Schaffer B, Nossif N, Shen T, Weissleder R, Brady TJ: Colloidal magnetic resonance contrast agents: Effect of particle surface on biodistribution. *J Magnetism Magnetic Mater* 122:383–386, 1993
26. Hancock WW, Lord RH, Colby AJ, Diamantstein T, Rickles FR, Dijktra C, Hogg N, Tilney NL: Identification of IL $2R^+$ T cells and macrophages within rejecting rat cardiac allografts, and comparison of the effects of treatment with anti-IL 2R monoclonal antibody or cyclosporin. *J Immunol* 138:164–170, 1987
27. Wang JJ, Hendrich KS, Jackson EK, Ildstad ST, Williams DS, Ho C: Perfusion quantitation in transplanted rat kidney by MRI with arterial spin labeling. *Kidney Int* 53:1783–1791, 1998
28. Racusen LC, Solez K, Colvin RB, Bonsib SM, Castro MC, Cavallo T, Croker BP, Demetris AJ, Drachenberg CB, Fogo AB, Furness P, Gaber LW, Gibson IW, Glotz D, Goldberg JC, Grande J, Halloran PF, Hansen HE, Hartley B, Hayry PJ, Hill CM, Hoffman EO, Hunsicker LG, Lindblad AS, Marcussen N, Mihatsch MJ, Nadasdy T, Nickerson P, Olsen TS, Papadimitriou JC, Randhawa PS, Rayner DC, Roberts I, Rose S, Rush D, Salinas-Madrigal L, Salomon DR, Sund S, Taskinen E, Trpkov K, Yamaguchi Y: The Banff 97 working classification of renal allograft pathology. *Kidney Int* 55:713–723, 1999
29. Soots A, Lautenschlager I, Krogerus L, Saarinen O, Ahonen J: An experimental model of chronic renal allograft rejection in the rat using triple drug immunosuppression. *Transplantation* 65:42–46, 1998
30. Shulze E, Ferrucci JT, Poss K, Lapointe L, Bogdanova A, Weissleder R: Cellular uptake and trafficking of a prototypical magnetic iron oxide label in vitro. *Invest Radiol* 30:604–610, 1995
31. Moore A, Weissleder R, Bogdanov A Jr: Uptake of dextran-coated monocrystalline iron oxides in tumor cells and macrophages. *J Magn Reson Imaging* 7:1140–1145, 1997
32. Harisinghani MG, Saini S, Weissleder R, Hahn P, Yantiss RK, Tempay C, Wood BJ, Mueller PR: MR lymphangiography using ultrasmall superparamagnetic iron oxide in patients with primary abdominal and pelvic malignancies: Radiographic-pathologic correlation. *Am J Roentgenol* 172:1347–1351, 1999
33. Kerr PG, Nikolic-Paterson DJ, Lan HY, Tesch G, Rainone S, Atkins RC: Deoxyspergualian suppresses local macrophage proliferation in rat renal allograft rejection. *Transplantation* 58:596–601, 1994
34. Yang NS, Wu LL, Nikolic-Paterson DJ, Ng YY, Yang WC, Lan HY: Local macrophage and myofibroblast proliferation in progressive renal injury in the rat remnant kidney. *Nephrol Dial Transplant* 13:1967–1974, 1998
35. Nadasdy T, Ivanyi B, Orvos H, Bodrogi T, Csajbok E, Marofka F, Ormos J: Recurrence of focal sclerosing glomerulonephritis in the kidney graft. *Orv Hetil* 130:2369–2373, 1989
36. Hughes J, Liu Y, Van Damme J, Savill J: Human glomerular mesangial cell phagocytosis of apoptotic neutrophils: Mediation by a novel CD36-independent vitronectin receptor/thrombospondin recognition mechanism that is uncoupled from chemokine secretion. *J Immunol* 158:4389–4397, 1997
37. Morozumi K, Thiel G, Albert FW, Banfi G, Gudat F, Mihatsch MJ: Studies on morphological outcome of cyclosporine-associated arteriolopathy after discontinuation of cyclosporine in renal allografts. *Clin Nephrol* 38:1–8, 1992